DOI 10.5162/sensor2017/D2.1

Printed embedded transducers: Fabrication, design and characterization of selected applications

Johannes Sell[1], Herbert Enser[2], B. Jakoby [2], M. Schatzl-Linder[2], B. Straußß[2], W. Hilber[1]
[1] Institute for Microelectronics and Microsensors, Johannes Kepler University Linz, Austria,
[2] R&D organic coatings, voestalpine Stahl GmbH, Linz, Austria
johannes.sell@jku.at

Abstract:
This contribution gives an overview on our recent work on printed embedded transducers. It is focused on the description of appropriate technologies as well as technological considerations for the integration of sensors and actuators into the coating of sheet metal. In particular, the integration of capacitive large area sensors, piezo- and pyroelectric layers and strain gauges is discussed. The devised concept has the potential to introduce additional functionality (e.g., in terms of sensors) to a variety of products without the need of significant changes to their existing implementation.

Key words: printed transducers, embedded transducers, printed sensors, industrial application.

Introduction

In recent years, enormous progress has been achieved in the development of functional inks and pastes. Today, a variety of nanoparticle- and flake-based inks and pastes (including silver and carbon) and conductive polymer inks and pastes (e.g., PEDOT:PSS) are commercially available. These materials can be used in additive deposition processes, e.g., ink jet printing, gravure offset printing, flexographic printing, screen printing or spray coating and enable the realization of printed electronics and transducers, e.g., polymer solar cells [1], OLEDs [2], RFID antennas [3], [4], piezoelectric sensors [5] capacitive gas sensors [6] or strain gauges [7]. Compared to state-of-the-art semiconductor fabrication processes, the printing technology is cost effective and enables a rapid transfer of new developments from laboratory to fabrication scale. In general, polymeric foils, glass or coated paper are used as substrate for printed electronics. The final printed circuitry and sensor components are then integrated into a product in successive assembly steps.

In our work, we take the next step of integration by omitting a dedicated substrate and using the surface of an existing product as substrate instead. This approach has the advantage that no further assembly steps are necessary and that no additional adhesive/adhesion layer is required. Furthermore, a variety of transducers can be embedded in virtually every surface which can be coated. As an example of the proposed concept, we illustrate the realization of printed embedded transducers on coated sheet steel.

Sheet metal as substrate

Sheet metal with a thickness ranging from 0,5 mm to 2 mm is used as substrate. The sheet metal is primed with a polyurethane or polyester primer with a thickness of between 5 µm and 20 µm. Due to the inherent surface roughness of the used sheet metal and the pigmentation of the applied primers, the surface roughness R_q of the substrate (given by the root-mean-squared deviation) is in the range of 1 µm. This is orders of magnitude higher than on other substrates, normally used for the realization of printed transducers [8]. The high surface roughness impedes the printing of very thin conductive layers and excludes certain applications of printed electronics, like, e.g., OLEDs, which require homogeneous, defect free layers with well-defined thicknesses. Uncoated paper, in general, is rougher than the organic primer layer. Despite of its rough surface, many applications, including light-emitting electrochemical cells [9] and loudspeakers [10], have been realized on uncoated paper. Further examples for printed electronics on paper are given in [11].

The chemical and physical properties of the primer layer are crucial for the selection of printing materials. The surface energy of the primers used on the metal sheets is in the range 28 mN m^{-1} – 33 mN m^{-1}. This is well below the surface energy of substrates commonly used for printed electronics, e.g., PET or polyimide [12] which both have surface energies close to 40 mN m^{-1}. For appropriate wetting of the substrate, it is crucial that the surface tension of the ink or paste is close to the surface energy of the primer. Commercially available ink and paste formulations are typically designed for the application on the above mentioned standard substrates. Therefore, wetting and adhesion problems can occur and have to be investigated thoroughly before further application. Furthermore, the chemical resistance of the primer to the ink's or paste's solvent has to be considered. The primer itself is thermally crosslinked and stable towards most solvents. However, solvents can still introduce swelling of the primer which might result in a loss of adhesion to the metal substrate.

Printing technology

Printing is an additive manufacturing technology which can easily be scaled from lab-to-fab and enables the low cost mass production of electronic components. A comprehensive review of the technologies used for printed electronics and their unique properties (resolution, printing speed, layer thickness, …) for the fabrication of sensors and electronics is given in [13].

The prototypes shown exemplarily in this work are fabricated using flatbed screen printing. The silver pastes (LOCTITE ECI1010 and LOCTITE EDAG PF 050) and the carbon paste (LOCTITE EDAG PR 406B) were received from Henkel, the PEDOT:PSS paste ORGACON EL-P3155 was obtained from AGFA and the P(VDF-TrFE) formulation was kindly provided by Joanneum Research.

Capacitive sensors on steel

The realization of embedded capacitive sensors on steel substrate was previously investigated [8]. As illustrated in Fig. 1, capacitive sensors can either be based on sensing the self-capacitance, i.e., the capacitance between sensor and the conductive substrate, or the mutual capacitance, i.e., the capacitive coupling between two conductive structures (e.g., interdigital electrodes).

For a large area application of embedded capacitive sensors on metallic substrate, several challenges have to be met. One of these challenges is the low thickness of the

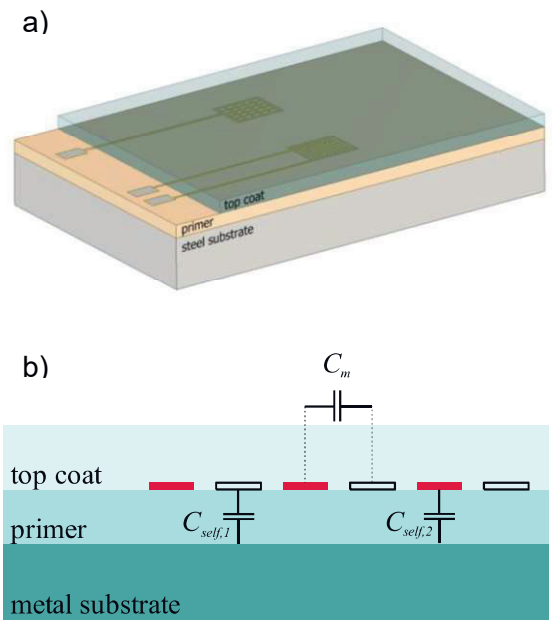

Fig. 1 a) Schematic layout of self (upper) and mutual (lower) capacitance based buttons; (b) cross section of a mutual capacitance based button with capacitive coupling schemas.

isolating primer layer and its high relative permittivity. Applied to a 20 µm primer, the self-capacitance per area is in the order of 300pF/cm². For a large area sensors, the offset self-capacitance may exceed the shift of the self-capacitance due to an interaction by orders of magnitude. Therefore, it may be difficult to resolve an interaction and, thus in general, it is advisable to use the mutual capacitance for the realization of large area capacitive sensors.

Another important aspect which has to be considered for the realization of large area sensors is the resistivity of the printed conductors. The resistivity results in a low-pass behavior which, strongly simplified, limits the frequency at which the interaction can be measured to $f_c = \frac{1}{2\pi R_L C_L}$, where R_L is the line

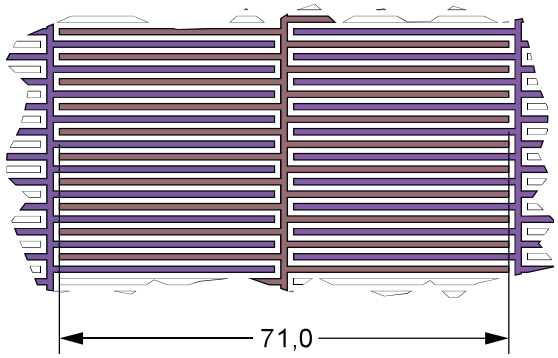

Fig. 2: Schematic description of the general layout of a large area capacitive sensor. The structure is repeated over an area of 260 mm x 1200 mm. The gap and the line width are 1 mm.

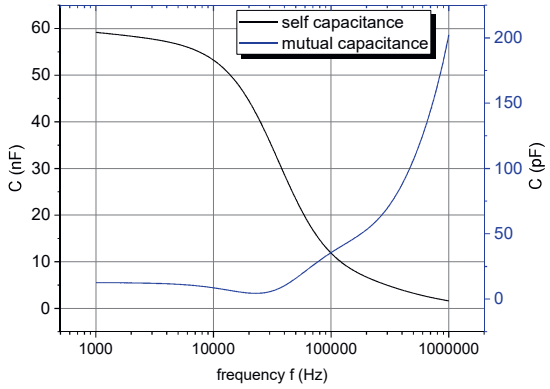

Fig. 3: Self-capacitance (left) of an electrode and mutual capacitance (right) of the same electrode with an adjacent electrode.

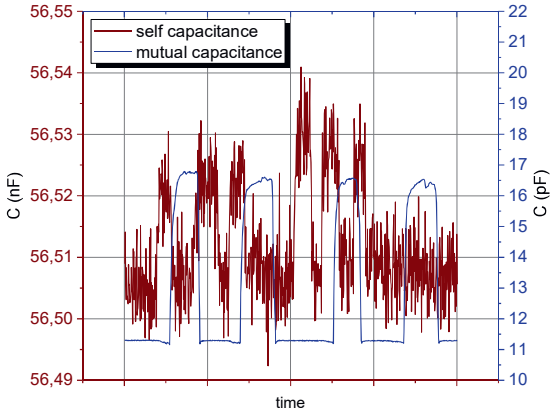

Fig. 4: Influence of a finger on the (left) self-capacitance and (right) mutual capacitance of a large area capacitive sensor. The capacitance was measured at 5 kHz with an Agilent 4294A impedance analyzer

resistance of the printed conductor and C_L is its overall capacitance. In practice, this restricts the choice of material for the realization of large area sensors to metal based polymer nanocomposites and the minimum reaction time, i.e., the time delay between an interaction and its detection, to milliseconds.

A schematic implementation of a prototype large area capacitive sensor can be seen in Fig. 2. It is based on interdigital electrodes with a line width and a gap of 1 mm respectively. This structure is repeated over an area of 260 mm x 1200 mm. In the prototype application, each electrode is 71 mm wide. This width is a tradeoff between the number of channels required for the readout of the sensor and the spatial resolution in horizontal direction. Depending on the available readout options, this value can, of course, be adjusted to the requirements of the target application.

Large area sensors were manually screen printed with a conductive silver paste (Henkel ECI1010) on a primed steel substrate with a primer thickness of 20 µm. A polyester mesh (SEFAR PET 1500) with a mesh number of 120/305-34 was used for the screen. The paste was cured in a continuous furnace at 110°C.

The electric characterization of the sensor was executed without further top coating of the sensor. Instead, the sensor areas was covered with two sheets of plastic foil with a total thickness of approximately 40 µm. The self-capacitance of the electrodes and the mutual capacitance of adjacent electrodes was determined with an Agilent 4294A impedance analyzer. For the measurement of the mutual capacitance, the steel substrate was connected to ground. Exemplarily, the self-capacitance of one of the electrodes and the mutual capacitance it features with an adjacent electrode is depicted in Fig. 3. Cleary, the large offset of the self-capacitance and the frequency dependence of the sensor can be seen.

The shift of the capacitance introduced by placing a finger on the sensor structure is shown in Fig. 4. The capacitance was measured with the impedance analyzer at 5 kHz. For the given sensor structure, primer and cover foil thickness the self-capacitance increases about 20 pF. The influence on the mutual capacitance is in the range of 5 pF. The offset capacitance of the mutual capacitance is only 11 pF whereas the offset capacitance of the self-capacitance measurement is in the range of 56 nF. Therefore, despite the higher absolute value, resolving the shift of the self-capacitance with the impedance analyzer is more difficult than resolving the shift of the mutual capacitance and requires additionally significant more averaging in order to achieve a reasonable sensor signal.

Embedded strain gauges

Strain gauges are widely used for the measurement of force, strain, and torque in components that are subject to mechanical stress. Using printing techniques, sensor implementations based on graphite [14], silver [15], PEDOT:PSS [16] and carbon nanotubes [17] have been demonstrated. In general, these strain gauges have been fabricated on polymeric substrate, e.g, polyimide [18], polyamide [16], or poly-dimethyl-siloxane (PDMS) [19].

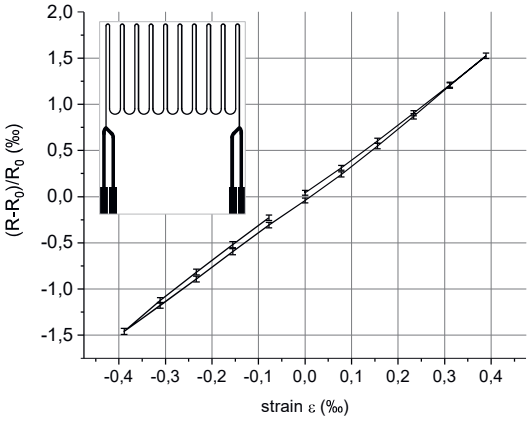

Fig. 5: Strain dependence of an embedded strain gauge, screen printed with carbon polymer thick film ink (Henkel Electrodag PR-406B). The response of the sensor was averaged over 172 deflection cycles. The standard deviation is indicated by error bars. The senor has a gauge factor or 3.8.

All these sensors have in common that the strain gauge is fixed to a test device by an adhesive layer. This adhesive layer impedes the direct measurement of strain on the test device as the mechanic properties of the adhesive are important for the perception of strain on an attached sensor. This issue can be solved by direct printing of a strain gauge sensors to the surface of a test device [20], [21].

Meander shaped strain gauges were embedded into the organic coating of sheet steel as explained in [21]. The response of such an embedded carbon based strain gauge can be seen in Fig. 5. For the characterization of the sensor, the steel substrate was clamped at one side. The strain gauge was positioned at the edge of the fixation where the maximum strain, introduced by a deflection on the other end of the steel substrate, occurs. The end of the steel substrate was deflected by ± 5 mm using a motorized stage. To ensure temperature stability during the measurements, the sample was placed in a climate chamber at 25 °C and 50 % relative humidity. The resistance of the sensors was recorded over 172 deflection cycles with a Keithley DMM7510 multimeter. A slight hysteresis and non-linearity can be seen in the sensor response. These effects will be subject to further investigations and publications.

Embedded piezo- and pyroelectric transducers

The polymer poly[(vinylidenefluoride-co-trifluoroethylene (P(VDF-TrFE)) enables the realization of flexible piezo- and pyroelectric transducers. Diluted in an appropriate solvent, it can be applied by many additive manufacturing processes, including, e.g., spray coating [22], inkjet printing [23], screen printing [24] and spin coating [25], [26]. Recent applications include the fabrication of ultrasonic transducers [27], loudspeakers [28] and piezo- and pyroelectric sensor-matrix on plastic foil [24].

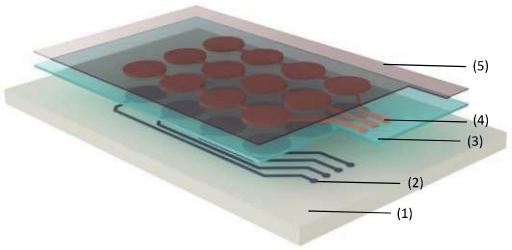

Fig. 6: Multilayer ferroelectric sensor stack design. (1) Substrate with organic coating. (2) Bottom electrode. (3) P(VDF-TrFE) ferroelectric intermediate coating. (4) Top electrode. (5) Organic top coating.

We have demonstrated the realization of the embedded piezo- and pyroelectric sensors in the organic coating of sheet steel [29]. In contrast to the sensors discussed above, the original primer-topcoat buildup has to be extended by three layers: a structured bottom electrode, a P(VDF-TrFE) layer and a structured top electrode (see Fig. 6). To generate the pyro- and piezoelectric properties of the P(VDF-TrFE) layer, high voltage poling, e.g., with a Sawyer-Tower circuit [30], is required. At peaks of the primer surface, very high electric field strengths may occur during the poling. To avoid electric breakdowns, the thickness of the P(VDF-TrFE) layer should be one order of magnitude higher than the root mean square surface roughness of the bottom electrode. The obtained piezoelectric coefficient after poling is strongly depending on the applied electric field strength. To ensure a homogeneous piezoelectric coefficient in the layer, a uniform film thickness is important.

A proof-of-principle realizations of an early versions of the concept is shown in Fig. 7. In this prototype, the P(VDF-TrFE) layer was spin coated on top of a steel substrate. The top electrodes were screen printed with PEDOT:PSS ink. The electric response was measured with the ADC input of a STM32F4 microcontroller. By moving a hot air gun over the sample the pyroelectric effect was demonstrated. As can be seen on the display in Fig. 7 (upper), voltage pulses are generated in all four sensor elements. The piezoelectric effect is demonstrated by pressing an electrode with a glove protected finger. The corresponding voltage peak can, again, be seen in the display (lower).

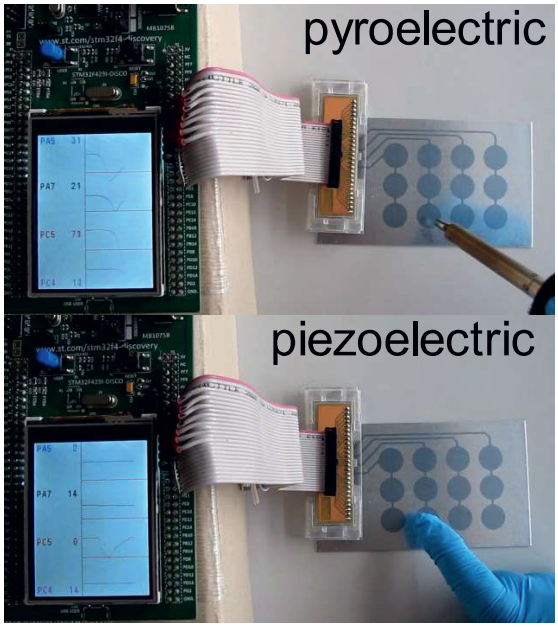

Fig. 7: Demonstration of the pyro- (upper) and piezoelectric (lower) properties of an early P(VDF-TrFE) based prototype. The voltage response of the sensor is recorded with the ADC input of a STM32F4 microcontroller. The sensor consist of steel substrate, P(VDF-TrFE) layer and PEDOT:PSS top electrodes.

Conclusion

- Selected implementations of embedded transducers in the organic coating of sheet metal were shown in this work.
- The devised concept has the potential to introduce additional functionality (e.g., touch, heat or strain sensing) to a variety of products without the need of significant changes to their existing implementation.

Acknowledgement

This work has been supported by the Linz Center of Mechatronics (LCM) in the framework of the Austrian COMET-K2 programme and the Austrian Research Promotion Agency (FFG - project no. 5834690).

References

[1] F. C. Krebs *et al.*, *Sol. Energy Mater. Sol. Cells*, vol. 93, no. 4, pp. 422–441, 2009.
[2] T. Minakata *et al.*, "R2R processed flexible OLEDs for lighting," in *Proc. SPIE 9566, Organic Light Emitting Materials and Devices XIX*, 2015, p. 95660J.
[3] M. Allen, C. Lee, B. Ahn, T. Kololuoma, K. Shin, and S. Ko, *Microelectron. Eng.*, vol. 88, no. 11, pp. 3293–3299, 2011.
[4] M. Jung *et al.*, *Electron Devices, IEEE Trans.*, vol. 57, no. 3, pp. 571–580, 2010.
[5] M. Zirkl *et al.*, *Adv. Mater.*, vol. 23, no. 18, pp. 2069–2074, 2011.
[6] U. Altenberend *et al.*, *Sensors Actuators, B Chem.*, vol. 187, pp. 280–287, 2013.
[7] M. Maiwald, C. Werner, V. Zoellmer, and M. Busse, *Sensors Actuators A Phys.*, vol. 162, no. 2, pp. 198–201, Aug. 2010.
[8] J. K. Sell, H. Enser, B. Jakoby, M. Schatzl-Linder, B. Strauss, and W. Hilber, *IEEE Sens. J.*, vol. 16, no. 19, pp. 7101–7108, 2016.
[9] A. Sandström, A. Asadpoordarvish, J. Enevold, and L. Edman, *Adv. Mater.*, vol. 26, no. 29, pp. 4975–4980, 2014.
[10] A. C. Hübler, M. Bellmann, G. C. Schmidt, S. Zimmermann, A. Gerlach, and C. Haentjes, *Org. Electron. physics, Mater. Appl.*, vol. 13, no. 11, pp. 2290–2295, 2012.
[11] D. Tobjörk and R. Österbacka, *Adv. Mater.*, vol. 23, no. 17, pp. 1935–1961, 2011.
[12] T. H. J. Van Osch, J. Perelaer, A. W. M. De Laat, and U. S. Schubert, *Adv. Mater.*, vol. 20, no. 2, pp. 343–345, 2008.
[13] S. Khan, L. Lorenzelli, and R. S. Dahiya, *IEEE Sens. J.*, vol. 15, no. 6, pp. 3164–3185, 2015.
[14] D. Zymelka, T. Yamashita, S. Takamatsu, T. Itoh, and T. Kobayashi, *Jpn. J. Appl. Phys.*, vol. 56, no. E5EC02, pp. 1–5, 2017.
[15] G. I. Hay, P. S. A. Evans, D. J. Harrison, D. Southee, G. Simpson, and P. M. Harrey, *IEEE Sens. J.*, vol. 5, no. 5, pp. 864–871, Oct. 2005.
[16] G. Latessa, F. Brunetti, A. Reale, G. Saggio, and A. Di Carlo, *Sensors Actuators, B Chem.*, vol. 139, no. 2, pp. 304–309, 2009.
[17] I. Kang, M. J. Schulz, J. H. Kim, V. Shanov, and D. Shi, *Smart Mater. Struct.*, vol. 15, no. 3, pp. 737–748, Jun. 2006.
[18] U. Lang, P. Rust, and J. Dual, *Microelectron. Eng.*, 2008.
[19] S. Khan, W. Dang, L. Lorenzelli, and R. Dahiya, *IEEE Trans. Semicond. Manuf.*, vol. 28, no. 4, pp. 486–493, 2015.
[20] J. Rausch, L. Salun, S. Griesheimer, and M. Ibis, *TEST Conf. 2011*, 2011.
[21] H. Enser *et al.*, "Printed strain gauges embedded in organic coatings," in *Procedia Eng.*, 2016, p. 4.
[22] R. Danz, B. Elling, A. Buchtemann, and P. Mirow, "Preparation, characterization and sensor properties of ferroelectric and porous fluoropolymers," in *11th International Symposium on Electrets*, 2002, pp. 199–202.
[23] R. I. Haque, R. Vié, M. Germainy, L. Valbin, P. Benaben, and X. Boddaert, *Flex. Print. Electron.*, vol. 1, no. 1, p. 15001, 2016.
[24] M. Zirkl *et al.*, *Adv. Mater.*, vol. 23, no. 18, pp. 2069–2074, 2011.
[25] Y.-Y. Choi *et al.*, *J. Mater. Chem.*, vol. 21, no. 13, p. 5057, 2011.
[26] H. J. Tseng, W. C. Tian, and W. J. Wu, *Sensors (Basel).*, vol. 13, no. 11, pp. 14777–14796, 2013.
[27] H. Ohigashi, K. Koga, M. Suzuki, T. Nakanishi, K. Kimura, and N. Hashimoto, *Ferroelectrics*, vol. 60, no. 1, pp. 263–276, Oct. 1984.
[28] A. C. Hübler, M. Bellmann, G. C. Schmidt, S. Zimmermann, A. Gerlach, and C. Haentjes, *Org. Electron. physics, Mater. Appl.*, vol. 13, no. 11, pp. 2290–2295, 2012.
[29] H. Enser, J. K. Sell, B. Jakoby, and W. Hilber, "Concept For Printed Ferroelectric Sensors On Coated Metallic Substrates," in *2016 IEEE SENSORS - Proc.*, 2016.

[30] C. B. Sawyer and C. H. Tower, *Phys. Rev.*, vol. 35, pp. 269–275, 1930.